# Chemoinformatics Analysis Identifies Cytotoxic Compounds Susceptible to Chemoresistance Mediated by Glutathione and Cystine/Glutamate Transport System $x_c^-$

Zunyan Dai,[†] Ying Huang,[‡] Wolfgang Sadee,[†] and Paul Blower[†,*]

*Program of Pharmacogenomics, Department of Pharmacology and the Comprehensive Cancer Center, College of Medicine, The Ohio State University, Columbus Ohio 43210, and Department of Pharmaceutical Sciences, College of Pharmacy, Western University of Health Sciences, Pomona, California 91766*

*Received August 8, 2006*

Glutathione detoxification has been broadly implicated in resistance to chemotherapy. This study explores the relationship between chemical structure and GSH-mediated chemoresistance. System $x_c^-$, the heterodimeric cystine/glutamate exchanger composed of SLC7A11 and SLC3A2, plays a role in maintaining cellular glutathione (GSH) levels. Previous results show that SLC7A11 expression negatively correlates with drug potency across the National Cancer Institute's 60 cell lines for compounds susceptible to GSH-mediated chemoresistance. The number of significant SLC7A11−drug correlations was much greater than those of other genes tested, suggesting that SLC7A11 plays a critical role. Approximately 15% of a curated set of 3045 compounds yielded significant negative SLC7A11 correlations. These compounds tend to contain structural features amenable to GSH reactivity, such as Mannich bases. In cell lines strongly expressing SLC7A11, the potency of selected compounds, was enhanced by inhibition of SLC7A11. This system provides a rapid screen for detecting susceptibility of anticancer drugs to GSH-mediated resistance.

## Introduction

Chemoresistance is a major cause of treatment failure in cancer patients. A systematic approach in the design and screening of new anticancer drugs is needed for identifying drug candidates among a series of congeners to avoid chemoresistance. Correlation analysis of gene expression in tumor cells with cytotoxic drug potency represents a useful tool in the study of chemoresistance.[1−7] Scherf et al. described a method for integrating large databases on gene expression and molecular pharmacology.[7] mRNA expression profiles measured with cDNA microarrays in the National Cancer Institute's 60 cell line panel (NCI-60) were correlated with patterns of growth inhibitory potencies of anticancer drugs. A strong negative correlation between expression of a gene and compound potency means that cells expressing higher levels of the gene are less sensitive to this compound. Therefore, negative correlations suggest chemoresistance mechanisms that can be tested experimentally.

Extending the methodology of Scherf et al.,[7] we have developed data mining techniques for identifying structural features of compounds showing activity patterns highly correlated with specific mRNA expression patterns.[8] The approach was also used to discover associations between compound classes and molecular targets for cancer chemotherapy.[8] Representative compounds are then used to search for correlated genes that could contribute to molecular mechanisms of drug action. This has led to discovery and experimental validation of novel gene drug correlations relevant to chemoresistance and -sensitivity.[4,9] The goal of the present study is to characterize the relationship between chemical structure and susceptibility to glutathione-mediated chemoresistance, exploiting the extensive collection of compounds already tested against the NCI-60 cell panel.

Multiple mechanisms can contribute to resistance to chemotherapy, including alterations of drug metabolism and transport, drug target, cell proliferation and cell death, and DNA repair mechanisms.[10,11] Glutathione (GSH[a]) detoxification has been implicated in resistance to standard chemotherapy agents such as cisplatin, doxorubicin, and melaphalan.[12] GSH is synthesized in two steps from the constituent amino acids L-glutamate, L-cystine, and glycine (Supporting Information Figure 1(a)). In the first and rate-limiting step, $\gamma$-glutamyl cysteine synthetase ($\gamma$-GCS, also known as glutamate-cysteine ligase, catalytic subunit; GCLC) catalyzes the coupling of L-cystine with the $\gamma$-carboxylic acid of L-glutamate. In the second step, glutathione synthetase catalyzes the coupling of $\gamma$-Glu-Cys with glycine to form GSH. GSH synthesis is regulated by three factors: activity of the rate-limiting $\gamma$-GCS, cysteine availability, and GSH feedback inhibition.[13] Increase in $\gamma$-GCS activity and stimulation of cysteine (transported as cystine) uptake generally increase intracellular GSH concentrations.[14] GSH protects against cellular damage caused by reactive oxygen species (ROS). In addition, many xenobiotics are susceptible to GSH conjugation. Driven by a reactive sulfhydryl group, GSH conjugation is a major detoxification pathway, particularly of electrophilic substances such as epoxides, Michael acceptors, halides, and heavy metals (Supporting Information Figure 1(b)).[15] GSH conjugation can occur spontaneously, for example with strong Michael acceptors, or is catalyzed by a family of GSH-S-transferases (GSTs).

To permit a chemoinformatics approach for defining structural features associated with GSH-mediated chemoresistance, one needs to identify the rate-limiting key processes in GSH

* Corresponding author. Paul Blower, Department of Pharmacology, The Ohio State University, 5072 Graves Hall, 333 West 10th Ave., Columbus OH 43210, phone: 614-688-5565, fax: 614-292-7232, e-mail: blower.7@osu.edu.

[†] The Ohio State University.

[‡] Western University of Health Sciences.

[a] Abbreviations: NCI, the National Cancer Institute; DTP, Developmental Therapeutics Program; BSO, buthionine sulfoximine; (*S*)-4-CPG, (*S*)-4-carboxyphenylglycine; FDR, false discovery rate; GSH, glutathione; $\gamma$-GCS, $\gamma$-glutamylcysteine synthetase (glutamate-cysteine ligase, catalytic subunit; GCLC); ROS, reactive oxygen species; SRB, sulforhodamine B; GSTP1, glutathione s-transferase pi; pGI50, $-\log_{10}(GI_{50})$. $GI_{50}$, the concentration causing 50% cell growth inhibition.

10.1021/jm060960h CCC: $37.00 
Published on Web 03/17/2007

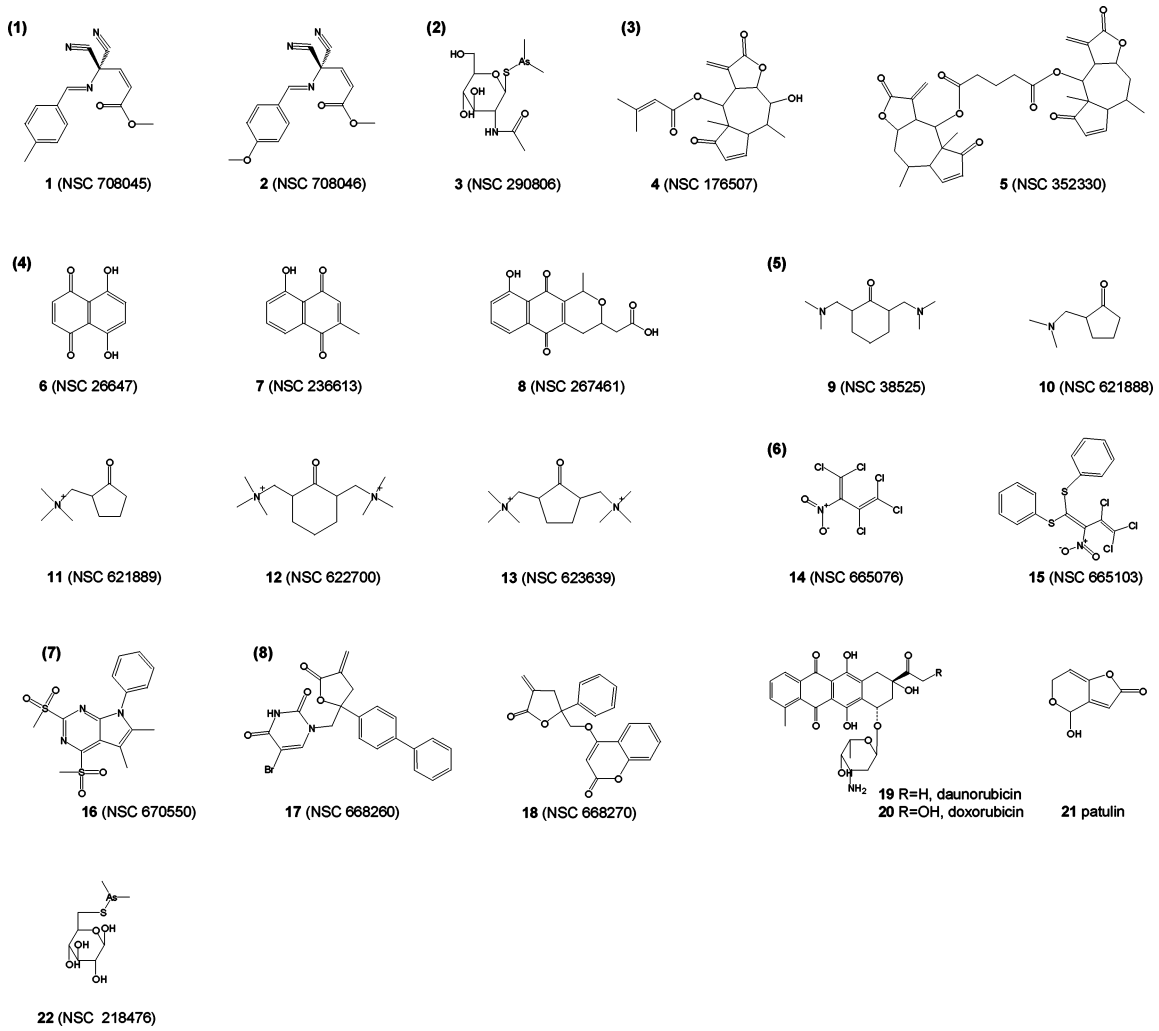


**Figure 1.** Chemical compounds selected to test the possibility of sensitization by inhibition of SLC7A11 or glutathione synthesis, compare with Table 4. NSC numbers (NCI assigned ID numbers) are listed for each compound, and the numbers in parentheses indicate compound class in Table 3. Information for all compounds, including chemical structure, chemical nomenclature, and test results, can be obtained from http://dtp.nci.nih.gov/dtpstandard/cancerscreeningdata/index.jsp. Compound **22** was not available from the NCI for testing.

metabolism. The first limiting step is the supply of cysteine by transport of cystine into the cells by the cystine/glutamate transporter, system $x_c^-$, consisting of SLC7A11 and SLC3A2 (or 4F2hc, 4F2 heavy chain, CD98). SLC7A11 (or xCT) encodes the transporter subunit,[16−18] exploiting high cellular levels of L-glutamate to drive import of L-cystine. Once inside the cell, cystine is rapidly reduced to cysteine, the limiting amino acid for GSH synthesis.[19] System $x_c^-$ plays an important role in regulating the intracellular GSH level, thought to mediate resistance against multiple drugs. Specifically, the $x_c^-$ amino acid transport system has been shown to maintain intracellular GSH and consequently results in cisplatin resistance in ovarian cancer cells.[20] We have previously reported that expression of system $x_c^-$ (SLC7A11 plus SLC3A2) in the NCI-60 correlates with chemoresistance by regulating cellular levels of glutathione,[9] making SLC7A11 a prime candidate for the present chemoinformatics study. Specifically, geldanamycin congeners yielded widely varying correlations with SLC7A11. Inhibiting or downregulating SLC7A11, or blocking GSH biosynthesis confirmed that glutathione mediates chemoresistance to geldanamycins with strong negative SLC7A11 correlations.[9,21]

The formation of $\gamma$-glutamyl cysteine, catalyzed by $\gamma$-GCS, is another limiting step that controls overall GSH supply, critical for cell survival and resistance to chemotherapeutic agents.[11,22] Transcriptional and posttranscriptional regulation strongly modulate $\gamma$-GCS activity,[23] a possible confounding factor in any expression−drug potency correlation. GSH depletion by L-buthionine-(*S*,*R*)-sulfoxime (BSO), a specific inhibitor of $\gamma$-GCS, is commonly used to reduce cellular levels of GSH, thereby increasing chemosensitivity, for example toward melphalan.[22,24] Moreover, BSO-induced GSH depletion increased oxidative stress and enhances the cytotoxic effects of 2-deoxy-D-glucose.[25] Clinical trials are ongoing to study the effectiveness of combining BSO with other chemotherapeutic agents.[26]

Glutathione-S-transferases (GSTs), a family of enzymes that catalyzes formation of GSH conjugates, have been implicated in the detoxification and resistance for a variety of chemotherapeutic drugs.[27] Highly expressed GSTs, such as GSTP1, in many tumors are potential therapeutic targets for inhibitors and GST-activated prodrugs.[28] Therefore, genes encoding GSTs are also potential candidates for inclusion with this chemogenomics study. However, GSTs contribute to drug resistance not only through direct detoxification, but also via MAP kinase-mediated apoptosis pathway.[27,28] Therefore, GSTs can render resistance to cytotoxic agents that neither form conjugates with GSH, nor serve as GST substrates.[27,28] In addition, the GST gene family contains numerous members, each with distinct substrate specificity and tissue expression. All these factors prevent their usage for defining structural features associated with GSH-

**Table 1.** Comparison of Correlation Coefficients for Selected Genes[a]

| gene[b] | frequency ($p < 0.05$) | frequency (adjusted $p < 0.05$) |
|---|---|---|
| SLC7A1 | 1 | 0 |
| SLC7A2 | 28 | 0 |
| SLC7A4 | 16 | 2 |
| SLC7A5[d] | 50 | 1 |
| SLC7A6 | 15 | 0 |
| SLC7A7 | 1 | 0 |
| SLC7A8 | 77 | 0 |
| SLC7A9 | 17 | 0 |
| SLC7A10 | 13 | 0 |
| SLC7A11 | 471 | 411 |
| ABCB1 | 276 | 21 |
| ABCC1 | 80 | 4 |
| GSTP1[c] | 47 | 8 |
| $\gamma$-GCS[c,d] | 153 | 37 |
| SLC7A11[c,d] | 592 | 520 |

[a] Frequency gives the number of negative compound−gene correlations with $r \leq -0.3$ and bootstrap $p$-value, $p \leq 0.05$ based on the 54 nonleukemia cell lines for the NCI 3K Set. Adjusted $p$-values were also calculated for multiple comparisons by the method of Benjamini and Hochberg.[32] [b] Except where indicated, all probes are from a custom spotted 70-mer microarray. [c] Probes from the Affymetrix U133A GeneChip. [d] These three genes had more than one probe on the microarrays, and the results are the mean values from probes for each gene.

mediated chemoresistance, by correlation between gene expression and drug potency.

In the present study, we have used gene−drug correlations to identify the optimal marker for defining GSH-mediated chemoresistance in the NCI-60 panel. While both $\gamma$-GCS and SLC7A11 showed significant gene−drug correlations, SLC7A11 yielded by far the most significant and frequent drug correlations, compared to all other genes tested. Results with geldanamycin analogs[9] have laid the foundation for rapid screening of anticancer drugs for optimal candidates that escape GSH-mediated chemoresistance. Here, we expand this approach to all chemical classes contained in a curated subset of 3045 (NCI 3K) test compounds. Using chemical features and compounds classes rather than single agents tested one at a time, this chemoinformatics approach reveals numerous compounds with highly significant SLC7A11 correlations (see Table 1) and common structural features associated with susceptibility to glutathione interaction (serving as Michael acceptors or as scavengers of oxygen radicals). *In vitro* cell culture studies confirmed a role of SLC7A11 in chemoresistance for negatively correlated compounds, employing inhibition of SLC7A11 using (*S*)-4-carboxyphenylglycine ((*S*)-4-CPG), and for comparison, inhibition of GSH synthesis using buthionine sulfoximine (BSO). These studies exemplify the utility of chemoinformatics in combination with rapid in vitro testing of drug candidates in cell lines expressing target genes.

## Results

**Gene−Drug Correlation Analysis of SLC7A11 and Related Genes.** We selected 3045 (NCI 3K) compounds from a curated subset of 7794 compounds following the criteria described in the method section. Correlation analysis between SLC7A11 expression in the NCI-54 nonleukemia panel (excluding all leukemia cell lines to avoid bias; leukemia cells are generally more sensitive to drugs than the other NCI-60 cells) and potencies of compounds in the NCI 3K anticancer agent database yielded 288 compounds with positive correlations ($r \geq 0.3$, $p \leq 0.05$) and >400 compounds with negative correlations ($r \leq -0.3$, $p \leq 0.05$; Table 1). Use of different mRNA expression datasets of the NCI-60 (Affymetrix, spotted oligonucleotide arrays, etc.) all yielded similar results with numerous correlations. We had previously validated SLC7A11 as a contributor to chemosensitivity (positive correlation coefficients) and resistance (negative correlation coefficients).[5,9] On the basis of this prior knowledge, we expected that these threshold values set reasonable limits with acceptable type I and II errors. The number of positive correlations suggests of a role for SLC7A11 in chemosensitivity, but is less striking. Therefore, this study focuses on negative correlations associated with chemoresistance. Taking all NCI 3K compounds together, the mean compound-SLC7A11 correlation coefficient was $m = -0.02$ and the standard deviation was $s = 0.26$).

To test whether the high number of compounds with significant negative SLC7A11 correlations is a true indicator of general chemoresistance factor, we selected all SLC7A gene subfamily members, $\gamma$-GCS, GSTP1, and the known chemoresistance genes *ABCB1* (MDR1) and *ABCC1* (MRP1) for comparison. For compounds in the NCI 3K set, Table 1 provides the number of compound−gene correlations with $r \leq -0.3$ and bootstrap $p$-value, $p \leq 0.05$, based on the 54 nonleukemia cell lines. While SLC7A11, $\gamma$-GCS, GSTP1, and ABCB1 had multiple negative correlations, the number of correlations with $r \leq -0.3$ is considerably higher for SLC7A11. Only 47 compounds showed $r \leq -0.3$ and bootstrap $p \leq 0.05$ for GSTP1, while $\gamma$-GCS correlated with an average 153 drugs, and ABCB1 with 276 drugs with $r \leq -0.3$ and bootstrap $p \leq 0.05$ (Table 1). Correcting for multiple hypotheses testing, necessary in particular with genes from which we have yet to validate any correlations by experiment, use of adjusted $p$ values did not significantly reduce the number of gene−drug correlations only for SLC7A11, whereas all other genes dropped dramatically. These results demonstrate that SLC7A11 yields robust negative correlations with numerous compounds associated with a general resistance mechanism likely mediated by glutathione.

**Correlations between SLC7A11 Expression and Compound Classes Clustered by Structure.** We used structure-based clustering of the NCI 3K to group compounds with significant correlation values by chemical features. This resulted in 747 classes of compounds, each containing similar chemical structures. Given the choice of clustering method, compound clustering depends on two factors: the set of molecular features or fingerprints used to describe compounds and the metric for measuring the degree of structural similarity between any pair of compounds. Both are potential sources of bias. The molecular descriptors used in this study are those defined in the LeadScope Structural Feature Hierarchy,[29] which is based on medicinal chemistry building blocks such as functional groups and heterocyclic fragments. The Tanimoto coefficient that we used to calculate molecular similarity is known to exhibit a bias based on molecular size or, more accurately, the bit density of the fingerprint.[30] Since the NCI-60 compounds have wide variation in size and complexity, this bias may affect clustering results. However, in our experience this procedure is effective for grouping structurally similar compounds typically found in databases of small molecule drug candidates.

Table 2 shows compound classes having high mean correlations, both negative (six classes) and positive (three classes), with SLC7A11 with $z$-scores of abs($z$) $\geq 5.0$. The column labeled Class in Table 2 contains a characterizing substructure for each compound class, showing that a diverse range of chemical structures appears to convey sensitivity toward the expression of SLC7A11. The pair of columns labeled SLC7A11 gives the mean correlation coefficient and $z$-score for the compounds in each class.

**Table 2.** Partial Results from Complete Linkage Clustering of NCI 3K[a]

| Class | Freq | SLC7A11[b] | | $\Delta pGI_{50}$ | |
|---|---|---|---|---|---|
| | | Mean | Z-Score | Mean | Z-Score |
| 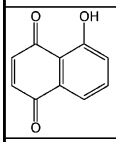 | 31 | -0.42 | -8.7 | -0.55 | -4.1 |
| 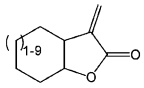 | 28 | -0.44 | -8.6 | -0.89 | -5.0 |
| 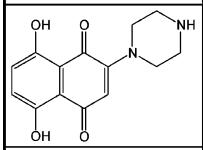 | 14 | -0.45 | -6.3 | -0.48 | -2.3 |
| 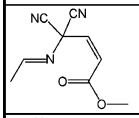 | 8 | -0.57 | -6.1 | -1.0 | -3.6 |
| 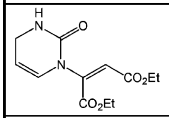 | 11 | -0.49 | -6.0 | -1.07 | -4.5 |
| 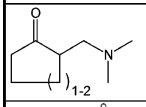 | 9 | -0.50 | -5.6 | -1.42 | -5.4 |
| 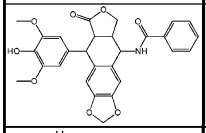 | 10 | 0.49 | 6.2 | 0.85 | 3.1 |
| 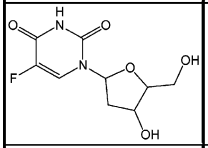 | 27 | 0.29 | 6.3 | 1.02 | 5.9 |
| 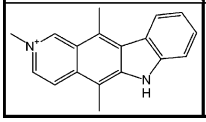 | 34 | 0.32 | 7.8 | 0.32 | 1.8 |

[a] The table shows nine classes with SLC7A11 *z*-scores with abs($z$) $\geq$ 5.0. For each class, a characterizing substructure is shown, class size, and two pairs of columns of biological data are given. The left pair of columns gives the mean compound-SLC7A11 correlation coefficient plus the *z*-score as calculated by eq 1. The correlation was calculated using the 54 nonleukemia cell lines. The right pair of columns gives analogous information for the $\Delta pGI_{50}$ value (HOP-62 − HOP-92); SLC7A11 mRNA expression is high in HOP-62 and low in HOP-92 cells.[9] [b] This pair of columns gives the mean compound-SLC7A11 Pearson correlation coefficient and *z*-score for the compounds in each class.

If there is a connection between chemoresistance and cellular levels of *SLC7A11*, we would expect to detect a difference in compound potency between cell lines with high and low expression of this gene. To corroborate compound−SLC7A11 correlations in Table 2, we calculated the difference in cytotoxic potency ($\Delta pGI_{50}$ value) between HOP-62 and HOP-92. Both are lung cancer cell lines with similar mRNA expression profiles,[9] while SLC7A11 mRNA expression is high in HOP-62 and low in HOP-92 cells. The pair of columns labeled $\Delta pGI_{50}$ give the mean difference and *z*-score for the compounds in each class. For the entire NCI 3K database, the mean $\Delta pGI_{50}$ value was $m = 0.05$ and the standard deviation was $s = 0.82$. Thus, for all 3K compounds the difference is not significant. However, for the compound classes in Table 2 with strong correlation coefficients, $\Delta pGI_{50}$ values between these two cell lines are consistent with SLC7A11 correlations across the entire NCI-60 panel. Compound classes with stronger negative (respectively, positive) correlations with SLC7A11 expression also show greater (respectively, lower) potency against HOP-92 compared to HOP-62.

**Selections of Chemical Compounds for Experimental Evaluation.** Using the filtered set of 471 compounds described above, we focused on compound classes that are negatively correlated with SLC7A11 expression to study the relationship between chemical structure and increased SLC7A11 expression associated with GSH-mediated chemoresistance.[9] Table 3 shows results from complete linkage clustering of 471 compounds which resulted in 180 classes with 80 singleton classes. Among eight classes with *z*-score values $z \leq -2.0$ for SLC7A11 (Table 3), class 1 contains aryl imines of dicyanocrotonates; class 2, thioarsenite derivatives of $\beta$-D-glucose; class 3, natural products such as fastigillin C (**4**) containing a fused α-methylene $\gamma$-lactone; class 4, hydroxynaphthoquinones; class 5, Mannich bases of cyclohexanone and cyclopentanone with 2-aminomethyl and 2,6-bis(aminomethyl) substituents; class 6, polychloronitrodienes; class 7, disulfonyl-substituted pyrrolopyrimidines; class 8, phenyl, aryloxymethyl-substituted α-methylene $\gamma$-lactones.

For each class, a characterizing substructure is shown, the class size and two pairs of columns of biological data. The left

**Table 3.** Partial Results from Complete Linkage Clustering of 471 Compounds[a]

| Class | | Freq | SLC7A11[b] | | $\Delta pGI_{50}$ | |
|---|---|---|---|---|---|---|
| | | | Mean | Z-Score | Mean | Z-Score |
| 1. Dicyanoacrylates | 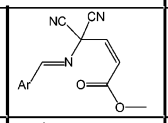 | 7 | -0.62 | -4.4 | -1.01 | -1.25 |
| 2. Arsenic thioglucoside | 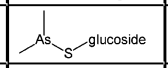 | 2 | -0.65 | -2.8 | -1.10 | -0.89 |
| 3. α-methylene γ-lactones | 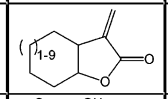 | 11 | -0.53 | -2.5 | -0.92 | -0.97 |
| 4. Hydroxyl-naphthoquinones | 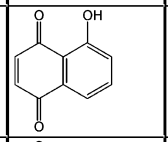 | 20 | -0.51 | -2.5 | -0.63 | 1.12 |
| 5. Mannich bases of aminomethyl-cyclopentanones & -cyclohexanones | 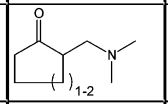 | 3 | -0.58 | -2.2 | -1.50 | -2.41 |
| 6. Polychloronitrodienes | 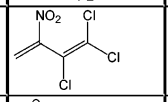 | 4 | -0.56 | -2.2 | -0.61 | 0.60 |
| 7. Pyrrolopyrimidines | 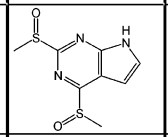 | 2 | -0.6 | -2.1 | -1.00 | -0.62 |
| 8. α-methylene γ-lactones | 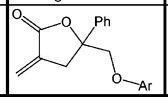 | 7 | -0.53 | -2.1 | -1.04 | -1.38 |

[a] The table shows eight classes with SLC7A11 *z*-scores $z < -2.0$. For each class, a characterizing substructure is shown, class size, and two pairs of columns of biological data are given. The left pair of columns gives the mean compound-SLC7A11 correlation coefficient and *z*-score, calculated using the 54 nonleukemia cell lines. The right pair of columns gives analogous information for the $\Delta pGI_{50}$ value (HOP-62 − HOP-92); SLC7A11 mRNA expression is high in HOP-62 and low in HOP-92 Cells.[9] [b] This pair of columns gives the mean compound-SLC7A11 Pearson correlation coefficient and *z*-score for the compounds in each class.

pair of columns gives the mean compound-SLC7A11 correlation coefficient plus the *z*-score as calculated by eq 1, with correlations derived from the 54 nonleukemia NCI-60 cell lines. The right pair of columns gives analogous information for the $\Delta pGI_{50}$ value (HOP-62 *versus* HOP-92). The table is sorted in increasing order by SLC7A11 *z*-score. For all 471 compounds, the mean SLC7A11 correlation coefficient was $m = -0.45$ ($s = 0.1$), and the mean $\Delta pGI_{50}$ value was $m = -0.76$ (standard deviation = 0.53). Guided by the entries in Table 3, we selected representative compounds from each class for experimental evaluation. The selected compounds are shown in Figure 1, representative of all chemical classes depicted in Table 3, with exception that compound **22** was not available from NCI for testing.

**Sensitization of Chemical Compounds by (*S*)-4-CPG.** Previous studies using inhibitors of SLC7A11 have shown that this transporter is critical for supplying cystine to the cell, needed for GSH biosynthesis, thereby conveying resistance to compounds interacting with GSH.[9] To determine whether inhibition of SLC7A11 transport function increases the potency of compounds with negative SLC7A11 correlations, we tested the compounds in Figure 1 and Table 4 with and without inhibition of SLC7A11 by (*S*)-4-CPG. Table 4 also gives the Pearson correlation coefficient with SLC7A11, calculated from 54 nonleukemia cell lines, and the $\Delta pGI_{50}$ value (HOP-62 versus HOP-92). For comparison, we included patulin (**21**), doxorubicin (**20**), and daunorubicin (**19**), previously shown to be affected by glutathione levels.[11,31] For all compound−SLC7A11 correlations, we calculated *p*-values using the Bootstrap procedure with 10 000 bootstrap samples and used the method of Benjamini and Hochberg[32] to control the false discovery rate (FDR).

**Patulin.** The mycotoxin patulin is highly electrophilic and readily forms adducts with cellular thiols such as GSH.[33] Exposure of cells to patulin leads to rapid depletion of GSH. Both GSH and cysteine decreased patulin-induced cellular injury, and cotreatment with BSO enhanced patulin toxicity.[31] Therefore, even though the correlation of patulin is modest ($r = -0.31$), we used patulin cytotoxicity to test the use of (*S*)-4-CPG for studying glutathione-modulated chemoresistance, for comparison with other test compounds. (*S*)-4-CPG-mediated inhibition of cystine import resulted in a 2.2-fold increase in sensitivity of HOP-62 cells to patulin (Table 4, and Figure 2 (d)).

**Anthracyclines: Doxorubicin and Daunorubicin.** Potency of doxorubicin and daunorubicin is known to be affected by glutathione level.[11] However, neither compound showed a significant correlation with SLC7A11, doxorubicin ($r = 0.29$, $p = 0.10$) and daunorubicin ($r = 0.20$, $p = 0.38$). In agreement with this, potencies of daunorubicin and doxorubicin were not significantly affected in HOP-62 and A549 cells by (*S*)-4-CPG (Table 4). This result indicates that in cell culture, GSH depletion does not mediate chemoresistance under the conditions of the experiments.

**γ-Lactones.** Two classes of α-methylene γ-lactones (Tables 3 and 4, classes 3 and 8) showed strongly negative correlations with SLC7A11 and large mean differences in cytotoxic potency between HOP-62 and HOP-92. Class 3 contains natural products such as compound **4** characterized by an α-methylene γ-lactone

**Table 4.** Tested Compounds[a]

| | | | | HOP-62 | | | A549 | | |
|---|---|---|---|---|---|---|---|---|---|
| class | compounds | PCC[b] | $\Delta pGI_{50}$ | (−) (*S*)-4-CP G | (+) (*S*)-4-CPG | fold | (−) (*S*)-4-CPG | (+) (*S*)-4-CPG | fold |
| patulin | **21** | −0.31 | −0.54 | 5.70 ± 0.02 | 6.05 ± 0.03 | 2.2 | N/A | N/A | N/A |
| daunorubicin | **19** | 0.20 | −0.11 | 7.54 ± 0.08 | 7.61 ± 0.05 | 1.2 | 7.54 ± 0.09 | 7.45 ± 0.09 | 0.81 |
| doxorubicin | **20** | 0.29 | 0.17 | 7.11 ± 0.08 | 7.32 ± 0.08 | 1.6 | 6.92 ± 0.04 | 6.79 ± 0.16 | 0.73 |
| 1 | **1** | −0.65 | −1.25 | 5.09 ± 0.02 | 5.19 ± 0.02 | 1.1 | 5.26 ± 0.01 | 5.39 ± 0.07 | 1.4 |
| | **2** | −0.65 | −0.97 | 5.28 ± 0.06 | 5.44 ± 0.17 | 1.5 | 5.71 ± 0.03 | 5.74 ± 0.03 | 1.1 |
| 2 | **3** | −0.64 | −1.24 | 5.79 ± 0.07 | 6.27 ± 0.12 | 3.0 | 6.51 ± 0.09 | 7.20 ± 0.06 | 2.0 |
| 3 | **4** | −0.46 | −0.66 | 6.50 ± 0.04 | 6.85 ± 0.02 | 2.2 | 6.59 ± 0.03 | 6.95 ± 0.02 | 2.3 |
| | **5** | −0.70 | −1.49 | 6.65 ± 0.07 | 6.93 ± 0.01 | 1.9 | 6.61 ± 0.01 | 6.74 ± 0.05 | 1.4 |
| 4 | **6** | −0.52 | −0.76 | 6.30 ± 0.06 | 6.62 ± 0.05 | 2.1 | N/A | N/A | N/A |
| | **7** | −0.70 | −1.08 | 5.01 ± 0.24 | 5.10 ± 0.58 | 1.2 | N/A | N/A | N/A |
| | **8** | −0.48 | −1.09 | 6.50 ± 0.03 | 6.68 ± 0.08 | 1.5 | N/A | N/A | N/A |
| 5 | **9** | −0.52 | −1.04 | 4.67 ± 0.01 | 5.18 ± 0.01 | 3.2 | 5.14 ± 0.01 | 6.14 ± 0.03 | 9.8 |
| | **10** | −0.47 | −1.27 | 5.90 ± 0.09 | 6.80 ± 0.06 | 7.9 | 5.24 ± 0.06 | 5.98 ± 0.13 | 5.4 |
| | **11** | −0.54 | −1.45 | 4.67 ± 0.03 | 5.26 ± 0.03 | 3.9 | 4.42 ± 0.05 | 5.37 ± 0.08 | 8.7 |
| | **12** | −0.66 | −1.72 | 5.24 ± 0.21 | 5.72 ± 0.43 | 3.0 | 5.63 ± 0.02 | 6.22 ± 0.06 | 3.8 |
| | **13** | −0.55 | −1.32 | 3.91 ± 0.03 | 4.04 ± 0.08 | 1.4 | 3.93 ± 0.02 | 4.07 ± 0.04 | 1.4 |
| 6 | **14** | −0.54 | −1.47 | 5.14 ± 0.11 | 5.15 ± 0.05 | 1.0 | 5.11 ± 0.02 | 5.22 ± 0.1 | 1.3 |
| | **15** | −0.62 | −0.17 | 5.86 ± 0.02 | 6.38 ± 0.03 | 3.3 | 6.18 ± 0.09 | 6.49 ± 0.06 | 2.0 |
| 7 | **16** | −0.62 | −1.02 | 5.53 ± 0.1 | 5.70 ± 0.03 | 1.5 | 5.76 ± 0.04 | 5.93 ± 0.02 | 1.5 |
| 8 | **17** | −0.51 | −2.14 | 5.99 ± 0.01 | 6.24 ± 0.02 | 1.8 | 6.02 ± 0.02 | 6.10 ± 0.03 | 1.2 |
| | **18** | −0.55 | −0.93 | 5.04 ± 0.04 | 5.36 ± 0.02 | 2.1 | 5.13 ± 0.05 | 5.28 ± 0.05 | 1.4 |

[a] Class (see compound classes in Table 3); PCC, Pearson correlation coefficient with SLC7A11 calculated from 54 nonleukemia cell lines; and $\Delta pGI_{50}$ value (HOP-62 − HOP-92). Groups of columns labeled HOP-62 and A549 give mean cytotoxicity $pGI_{50}$ with and without inhibition of SLC7A11 by (*S*)-4-CPG, fold is the $GI_{50}$ ratio of (−)(*S*)-4-CPG/(+)(*S*)-4-CPG. [b] FDR-adjusted p-values for all compound-SLC7A11 correlations had values $p < 0.0001$ except for patulin, $p = 0.138$; doxorubicin, $p = 0.096$; daunorubicin, $p = 0.380$; compound **4**, $p = 0.008$; compound **8**, $p = 0.004$; compound **18**, $p = 0.002$.

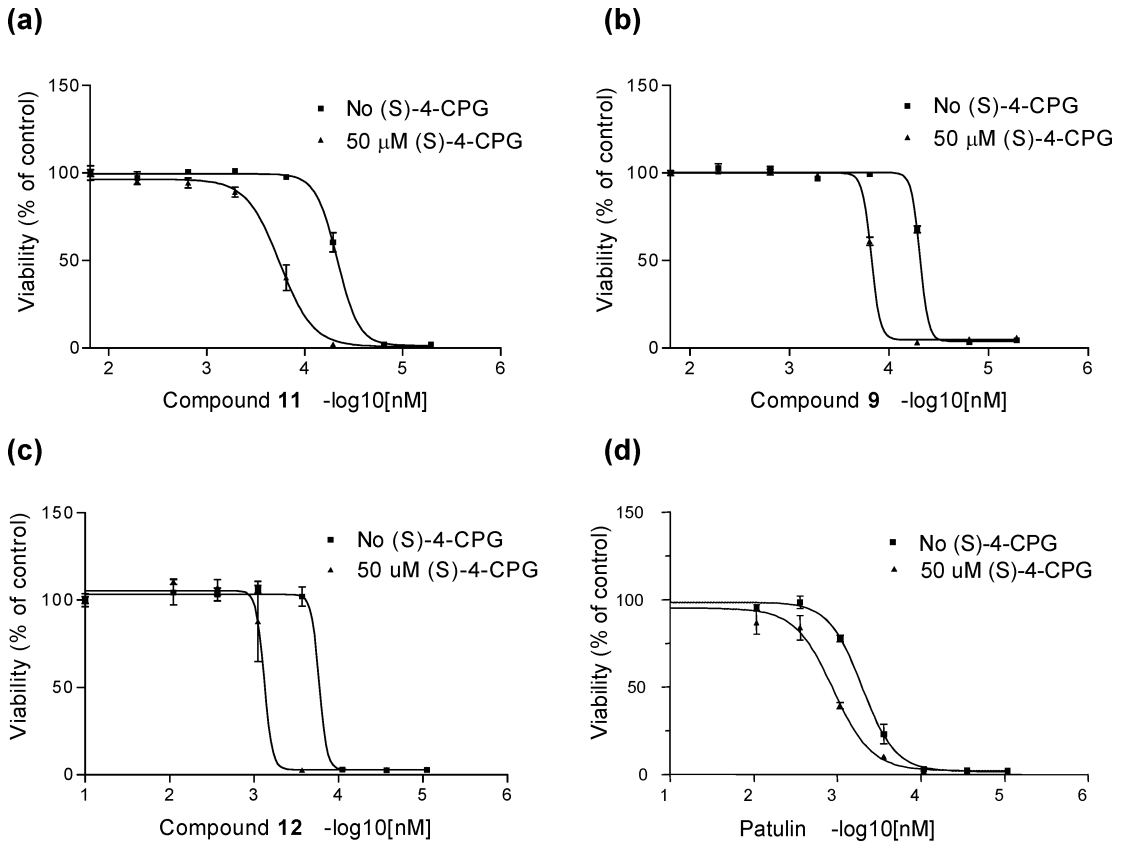


**Figure 2.** Dose response curves for selected compounds showing effects of inhibition of SLC7A11 by (*S*)-4-CPG in HOP-62 cells.

fused to a 6−14-membered carbocycle, and class 8 compounds typically have phenyl, aryloxymethyl substituents on the lactone ring. In all cases, the α-methylene moiety in both classes is unsubstituted making the electrophilic $CH_2{=}C{-}C{=}O$ fragment especially susceptible to Michael addition by GSH because of minimal steric hindrance. The four compounds tested in this study were modestly sensitized by (*S*)-4-CPG: a 2-fold difference for HOP-62 cells and a 1.6-fold difference for A549, both cells with high expression of SLC7A11 (Table 4). However, congeners of this class with the most negative correlations were not available from the DTP repository.

**Mannich Bases.** Mannich bases of cyclohexanone and cyclopentanone with 2-aminomethyl and 2,6-bis(aminomethyl) substituents (Table 3 and 4, class 5) were first synthesized by Dimmock et al.[34] For several Mannich bases, **9**, **10**, **11**, **12**, and **13**, we compared sensitivity in HOP-62 and A549 cells with

**Table 5.** Sensitization of Cytotoxic Compounds by (*S*)-4-CPG and BSO[a]

| compounds | cell lines | (−) (*S*)-4-CP G | (+) (*S*)-4-CPG | fold | (−) BSO | (+) BSO | fold |
|---|---|---|---|---|---|---|---|
| | | Class 3. α-Methylene γ-Lactones | | | | | |
| **4** | HOP-62 | 6.50 ± 0.04 | 6.85 ± 0.02 | 2.2 | 6.11 ± 0.02 | 6.27 ± 0.04 | 1.4 |
| | A549 | 6.59 ± 0.03 | 6.95 ± 0.02 | 2.3 | 6.27 ± 0.09 | 6.77 ± 0.16 | 3.2 |
| **5** | HOP-62 | 6.65 ± 0.07 | 6.93 ± 0.01 | 1.9 | 6.68 ± 0.01 | 6.78 ± 0.02 | 1.3 |
| | A549 | 6.61 ± 0.01 | 6.74 ± 0.05 | 1.4 | 6.38 ± 0.01 | 6.72 ± 0.02 | 2.2 |
| | | Class 5. Mannich Bases of Aminomethylcyclopentanones and -cyclohexanones | | | | | |
| **9** | HOP-62 | 4.67 ± 0.01 | 5.18 ± 0.01 | 3.2 | 4.71 ± 0.01 | 5.13 ± 0.01 | 2.6 |
| | A549 | 5.14 ± 0.01 | 6.14 ± 0.03 | 9.8 | 5.15 ± 0.02 | 5.65 ± 0.03 | 3.2 |
| **10** | HOP-62 | 5.90 ± 0.09 | 6.80 ± 0.06 | 7.9 | 4.71 ± 0.08 | 5.59 ± 0.07 | 7.7 |
| | A549 | 5.24 ± 0.06 | 5.98 ± 0.13 | 5.4 | 5.83 ± 0.02 | 6.90 ± 0.02 | 11.7 |
| **11** | HOP-62 | 4.67 ± 0.03 | 5.26 ± 0.03 | 3.9 | 4.74 ± 0.11 | 5.43 ± 0.07 | 4.9 |
| | A549 | 4.42 ± 0.05 | 5.37 ± 0.08 | 8.7 | 4.59 ± 0.03 | 5.10 ± 0.02 | 3.3 |
| **12** | HOP-62 | 5.24 ± 0.21 | 5.72 ± 0.43 | 3.0 | 5.26 ± 0.05 | 5.70 ± 0.03 | 2.7 |
| | A549 | 5.63 ± 0.02 | 6.22 ± 0.06 | 3.8 | 5.65 ± 0.02 | 6.11 ± 0.02 | 2.9 |
| **13** | HOP-62 | 3.91 ± 0.03 | 4.04 ± 0.08 | 1.4 | 3.974 ± 0.06 | 4.13 ± 0.06 | 1.4 |
| | A549 | 3.93 ± 0.02 | 4.07 ± 0.04 | 1.4 | 3.94 ± 0.04 | 4.11 ± 0.01 | 1.5 |

[a] The values are $pGI_{50}$. [b] Fold is the $GI_{50}$ ratio of (−)(*S*)-4-CPG/(+)(*S*)-4-CPG or (−)BSO/(+)BSO.

and without inhibition of cystine import by (*S*)-4-CPG. These compounds showed the greatest sensitivity to GSH depletion with differences ranging from 1.4- to 9.8-fold for both cell lines (Table 4 and Figure 2). Moreover, this class of compounds displayed very steep dose−response curves, approaching a step function.

**Arsenic Compounds.** Cellular GSH content has a decisive effect on apoptosis induced by arsenic trioxide ($As_2O_3$).[35−38] In our studies with the NCI-54 nonleukemia panel, arsenic trioxide showed negative correlations with SLC7A11, $r = -0.37$. In addition, a small subgroup of two thioarsenite derivatives of β-D-glucose compound **3** and compound **22** showed strongly negative correlations with SLC7A11; compound **3**, $r = -0.64$, and compound **22**, $r = -0.66$. Furthermore, both compounds showed differences in cytotoxic potency between HOP-62 and HOP-92; compound **3**, $\Delta pGI_{50} = -1.24$, and compound **22**, $\Delta pGI_{50} = -0.95$. We compared sensitivity to compound **3** in HOP-62 and A549 cells with and without inhibition of cystine import by (*S*)-4-CPG. HOP-62 showed a 3-fold increase in sensitivity in the presence (*S*)-4-CPG, and A549 showed 2-fold increase, indicating that GSH is at least partially responsible for chemoresistance to compound **3** in these cell lines.

**Other Classes.** Members of other class such as dicyanoacrylates (Table 3 and 4, Class 1), hydroxynaphthoquinones (Table 3 and 4, Class 4), polychloronitrodienes (Table 2 and 3, Class 6), and pyrrolopyrimidines (Table 3 and 4, Class 7) showed moderate sensitization by (*S*)-4-CPG with potency ratios for HOP-62 cells ranging from 1.1 to 2.1 (Table 4). An exception was the nitrodiene compound **15** containing the Ph−S−C═C−$NO_2$ fragment which shows a 3.3-fold sensitization in HOP-62 cells. This is probably in equilibrium with GS-C═C−$NO_2$ through Michael addition/elimination. The other tested nitrodiene compound **14** containing a $Cl_2C$═C−$NO_2$ fragment showed no sensitization in HOP-62 cells.

**γ-GCS Inhibitor BSO Shows Similar Sensitization Pattern as That of (*S*)-4-CPG.** We compared the sensitization effect of (*S*)-4-CPG and BSO because the two inhibitors function through different mechanisms to inhibit glutathione synthesis (Supporting Information Figure 1(a)). BSO, the inhibitor of γ-glutamylcysteine synthetase (γ-GCS), has been frequently used to study GSH-mediated chemoresistances, while (*S*)-4-CPG, inhibitor of cystine transport, has been less well studied. In general, we found that (*S*)-4-CPG is as effective as BSO in sensitizing cells to chemotherapeutic compounds subject to GSH-mediated resistance (Table 5 and Supporting Information Figure 2). For example, both (*S*)-4-CPG and BSO significantly shifted the potency of the Mannich bases (Tables 4 and 5, class 5) in HOP-62 and A549 lung cancer cell lines.

**mRNA Expression of SCL7A11 Has More Predictive Power Than That of γ-GCS**. Correlation analysis between γ-GCS expression in the NCI-54 nonleukemia panel yielded an average 153 out of 3045 (NCI 3K) compounds with negative correlations ($r \leq -0.3$, $p \leq 0.05$). Among these 153 compounds, approximately 106 compounds overlapped with the 471 compounds negatively correlated with SLC7A11. Moreover, the correlation between all Pearson correlation coefficient *r* values of γ-GCS and SLC7A11 (3045 compounds) was 0.65. This result demonstrates that mRNA expression profiles of both γ-GCS and SLC7A11 predict similar chemoresistance profiles, consistent with a common effect on GSH homeostasis, although by different mechanisms. We further evaluated the predictive power of γ-GCS for ten compounds that were sensitized by (*S*)-4-CPG more than twofold (Table 4) in HOP-62 cells. Only two of the ten compounds showed Pearson correlation coefficients $r \leq -0.3$ with γ-GCS (supplemental Table 1). This indicated that mRNA expression of γ-GCS is a less suitable marker for predicting GSH-mediated chemoresistance, requiring strongly varying expression in different cells lines. Expression of these two genes across the 54 nonleukemic cell lines displayed only a moderate Pearson correlation ($r = 0.47$). Taken together, the γ-GCS−drug correlations strongly support the validity of this approach for testing GSH-mediated chemoresistance but also demonstrate the superior properties of SLC7A11 expression profiles for the present study.

## Discussion

With cellular concentration in the 1−10 mM range, glutathione is the most abundant endogenous agent protecting cells from oxidative stress and electrophilic xenobiotics or their metabolites. Glutathione confers resistance to some chemotherapeutic agents, including cisplatin, melphalan, doxorubicin, daunorubicin, and arsenic trioxide.[11] To identify chemical compounds and chemical structures susceptible to GSH-mediated chemoresistance, we used chemoinformatics applied to a panel of 3045 (NCI 3K) anticancer compounds previously tested against the NCI-60. These were selected to display variable potencies across the NCI-60 cell lines to enhance the power of correlation analysis with mRNA expression profiles. We employed three genes, SLC7A11, γ-GCS, and GSTP1, in the GSH synthesis and detoxification process known to contribute to GSH-mediated chemoresistance. Previous study confirmed

that correlation of SLC7A11 expression with drug potency across NCI-60 identified GSH-mediated resistance to geldanamycin.[9] Given the preponderance of SLC7A11 correlations in Table 1, neither $\gamma$-GCS or GSTP1 is a viable alternative to SLC7A11 as a marker for GSH-mediated resistance. However, overlapping gene−drug correlations between $\gamma$-GCS and SLC7A11 support the validity of the approach, while GSTP1 mediates additional mechanisms unrelated to GSH.

**SLC7A11 mRNA Expression as a Predictor for GSH-Mediated Chemoresistance.** System $x_c^-$ plays an important role in maintaining cellular GSH levels and mediating chemoresistance to cytotoxic agents. The present study is the first to attempt a large-scale characterization of the chemical structures conveying GSH-mediated chemoresistance to drug candidates. Using the expression of SLC7A11 as the independent variable, we find that approximately 15% (471 of 3045) of the compounds show highly significant negative SLC7A11 correlations (411 FDR-adjusted $p$-values of $p < 0.05$). While this threshold value would still allow for inclusion of multiple false positive correlations, this is mitigated by our use of compound classes, providing additional supportive evidence for true correlations. Therefore, this stringency is appropriate for the present study. The first six classes in Table 2, which surveys the full curated NCI 3K database, shows compound classes with high negative mean compound-SLC7A11 correlations and large mean difference in cytotoxic potency between HOP-62 (which expresses high levels of SLC7A11) and HOP-92 (low levels). The latter provides an additional means for testing the relevance of the correlations. A large portion of these compounds possess structural features associated with susceptibility to glutathione-mediated resistance, further strengthening the hypothesis that glutathione is involved in chemoresistance.

A significant correlation between gene expression and drug activity is not a causative relationship. For instance, similar expression of two genes in the 54 cell lines would generate significant Pearson correlation coefficients for both of them; only one of them might be the cause of correlations. In addition, multiple factors might contribute to chemoresistance to one single compound. Therefore, experimental validation of significant correlation is necessary to establish the causative effect. We first validated the Pearson correlation coefficients for known chemical compounds, including patulin, daunorubicin, and doxorubicin. This was achieved by measuring the shift of compound potencies against cell lines strongly expressing SLC7A11, in the presence and absence of inhibitors of SLC7A11 and $\gamma$-GCS. The results were consistent with the negative correlation between patulin and SLC7A11 expression. Even though GSH is thought to affect the potency of anthracyclines, no significant correlations were observed for doxorubicin and daunorubicin. In agreement with this, inhibition of SLC7A11 did not affect drug potency significantly, similar to previous findings that BSO enhances the toxicity of doxorubicin by only 1.5 fold in MCF-7 breast cancer cells.[39] Similarly, the sensitization of cisplatin by glutathione inhibition is small (<2 fold).[9] Possibly multiple mechanisms contribute to the resistance of doxorubicin, daunorubicin, and cisplatin,[11,40] so that in the cells tested GSH-mediated chemoprotection plays only a minor role. Alternatively, *in vitro* cell culture conditions, allowing free oxygen access and providing ample nutrients, may not be optimal for testing GSH-mediated chemoresistance for all compounds in the NCI 3K panel.

We next tested the correlations for compounds not previously known to be related to GSH-mediated chemoresistance. We clustered the 471 compounds into different classes to select compounds for testing. From the eight classes listed in Table 3, we were able to obtain 18 compounds (Table 4) from the National Cancer Institute's Developmental Therapeutics Program (DTP). SLC7A11 inhibition sensitized 14 of them by at least 1.5 fold. In contrast to the known drugs, such as doxorubicin, daunorubicin, and cisplatin, which showed less than 2-fold sensitization due to multiple factors affecting their potency, 9 out of 18 tested compounds (50%) were sensitized by at least 2-fold. These 9 compounds were in 6 out of 8 chemical classes tested. For example, compound **3** is an arsenic compound that was sensitized 3-fold. Another arsenic compound, arsenic trioxide, is an ancient drug that has been proved recently to be a choice for the treatment of hematological malignancies,[41] and its potency was also affected by cellular gluthione level.[35−38] Although not currently found in clinical anticancer agents, Mannich bases, as a group of compounds, were significantly sensitized and have been tested as potential anticancer reagents.[34,42] In addition, Mannich bases are being studied as therapeutic compounds for many other purposes, including antitubercular,[43] antifungal,[44] anti-HIV,[45] and immunosuppressive[46] /anti-inflammatory agents. The role of glutathione-mediated chemotherapeutic resistance to those compounds is worth further study. In summary, our results show that a strong negative correlation with SLC7A11 is a reliable indication that a compound may be subject to glutathione-mediated chemoresistance. However, it is not expected that all the compounds selected based on the correlation analysis will be sensitized significantly, since the correlation values were derived from 54 cell lines, and factors influencing chemoresistance may vary with each cell line and with each compound or compound class. Differences in critical proteins involved in mediating cytotoxicity and resistance between specific cell lines and compounds could account for the less than quantitative relationship between correlation values and the extent of sensitization by GSH depletion. Therefore, some compounds with strongly negative SLC7A11 correlations and large $\Delta pGI_{50}$ values may show only modest sensitization by inhibition of SLC7A11 in any given cell type.

The last three classes in Table 2 include compounds with high positive mean SLC7A11 correlations and increased cytotoxic potency in HOP-62 compared to HOP-92. Both factors suggest that increased SLC7A11 expression enhance cellular sensitivity to these compounds. We have previously shown that L-alanosine is sensitized by SLC7A11 expresssion, serving as a cellular entry system for the drug.[9] However, it is unlikely that active transport into the cells is involved for the compounds in Table 2 since their chemical structures are unlikely substrates for the amino acid transporter system $x_c^-$. In some instances, conjugation with GSH has been shown to form toxic adducts, for example with vicinal dihaloalkanes such as dichloromethane.[47,48] We did not pursue these compound classes in this study but focused on the more abundant compounds where system $x_c^-$ appears to act as a chemoresistance factor.

**Mechanisms of GSH-Mediated Resistance for Chemical Compounds Tested in the Current Study.** Several compound classes showing strong negative correlations with *SLC7A11* contain the reactive Michael acceptor $CH_2{=}C{-}C{=}O$ substructure which is known to preferentially alkylate thiols in contrast to amino and hydroxyl groups.[34] These compounds could readily form adducts with GSH. This supports the hypothesis that GSH provides a chemoresistance mechanism that desensitizes *SLC7A11*-expressing cells such as HOP-62. Class 5 in Tables 3 and 4 are Mannich bases of cyclohexanone and cyclopentanone with 2-aminomethyl and 2,6-bis(aminomethyl) substit-

uents which were first synthesized by Dimmock et al.[34] These compounds are thought to undergo deamination to the reactive Michael acceptor $CH_2{=}C{-}C{=}O$ substructure. Thus, cytotoxicity of these Mannich bases may be the result of protein adduct formation or glutathione depletion, or both. The reaction of Mannich bases with GSH was shown to require a GST, such as GSTP1, but not in its absence.[49]

A striking feature of the dose−response curves for all tested members of the Mannich base class is the precipitous drop in cell viability over a small dosage range, both in the presence or absence of inhibitors (Figure 2 and Supporting Information Figure 2). Within a 2-fold to 3-fold dosage range, cell viability drops from near 100% viability to near 0% viability. Possibly, GSH maintenance collapses at a given drug concentration, at which point the cell is no longer protected. The biological basis of this phenomenon requires more detailed experimental study.

Quinones are well represented in the NCI 3K set, with 266 compounds, and many show strong negative correlations with SLC7A11. In addition to acting as Michael acceptors, quinones are redox-active molecules that can produce reactive oxygen species (ROS), such as superoxides and hydroxyl radicals. These reactive species can, in turn, cause peroxidation of lipids, oxidation of macromolecules, and DNA strand breaks. GSH can detoxify some quinones by reduction and break the redox cycling involved in cell damage. However, quinones with different structures display varying SLC7A11 correlations. For example, in the geldanamycin family, even small changes in a substituent on the quinone ring can substantially alter GSH-mediated resistance and sensitivity to SLC7A11 inhibition, reflected by corresponding correlation coefficients (Huang et al., unpublished data). The anthracyclines we tested here (Table 4), doxorubicin and daunorubicin, have nonsignificant correlation coefficients with SLC7A11 and showed only slight sensitization and were largely unaffected by inhibition of SLC7A11 in HOP-62 and A549. In contrast, the simple hydroxynaphthoquinones (class 4) have strongly negative SLC7A11 correlations but also showed only modest sensitization by inhibition of SLC7A11. We conclude that SLC7A11 correlations are indicators of GSH-sensitivity of the implicated compounds, but the correlations are not always predictive in a quantitative fashion, owing to differences in cell type studied and incubation conditions.

Cellular GSH content has a decisive effect on apoptosis induced by arsenic trioxide ($As_2O_3$).[35−38] Increases of GSH content decrease the sensitivity to $As_2O_3$ whereas depletion increases sensitivity. A mouse model of acute myeloid leukemia using HL-60 cells was shown to develop acquired resistance to $As_2O_3$.[37] This was partly attributable to the increased cellular GSH because drug resistance could be reversed with BSO treatment. The twofold increase in potency with SLC7A11 inhibition observed for the thioarsenite derivative of $\beta$-D-glucose that we tested, compound **3**, is likely the result of GSH displacing the thioglucoside to form GS-$AsMe_2$ which may be mediated by a GST.[27]

**SLC7A11 as a Potential Therapeutic Target.** The role of glutathione and related enzymes in chemoresistance has led to GSH depletion as a strategy for improving cancer chemotherapy.[11,50] For example, the $\gamma$-GCS inhibitor buthionine sulfoximine (BSO) and melphalan are being coadministrated and evaluated in clinical trials for the treatment of children with resistant or recurrent neuroblastoma (http://www.clinicaltrials.gov; Identifier: NCT00005835). Our study supports the notion that inhibition of glutamate/cystine transport by (*S*)-4-CPG is another effective strategy for overcoming GSH-mediated chemoresistance.[51] A number of potent glutamate/cystine transporter system inhibitors, including (*S*)-4-CPG and L-quisqualate, have been identified[21] and have potential as chemotherapeutic sensitizers.

In conclusion, our analysis provides a large-scale approach for identifying candidate compounds that are likely to be affected by GSH-mediated chemoresistance. It also provides a rapid means for testing GSH-mediated chemoresistance *in vitro*. Our chemoinformatics approach has revealed numerous compounds with highly significant SLC7A11 correlations and structural features associated with susceptibility to glutathione-mediated resistance. These studies exemplify the utility of chemoinformatics in combination with rapid in vitro testing of drug candidates in selected cell lines expressing the target gene. It can be applied to other genes or gene families for studying structure−activity relationships and guiding the selection of candidate anticancer drugs.

## Methods

**Chemoinformatics Methods.** To analyze gene expression−chemical structure relationships, the September 2003 release of the National Cancer Institute's (NCI) antitumor drug screening database was used. The data were obtained from the NCI's Developmental Therapeutics Program (DTP) website (Human Tumor Cell Line Screen: http://dtp.nci.nih.gov/docs/cancer/cancer_data.html) containing nonconfidential screening results and chemical structural data from the NCI's Developmental Therapeutics Program. For each compound and cell line, growth inhibition after 48 h of drug treatment had been assessed from changes in total cellular protein using a sulforhodamine B assay.[9] The data provide $pGI_{50}$ ($-\log(GI_{50})$ values for each compound−cell line pair ($GI_{50}$, the concentration causing 50% growth inhibition). From this data, we obtained a curated subset of 7794 compounds from colleagues at the NCI.[52] Compounds were selected as follows:

For those drugs that had $pGI_{50}$ values recorded at multiple concentration ranges, only the value at the best concentration range was selected. The best concentration range was chosen as the one containing the greatest number of values in the range:

$$[\text{low concentration} + 0.2, \text{high concentration} - 0.2]$$

In other words, values close to either endpoint were discounted. Compounds with fewer than 30 values were excluded. Finally, we selected compounds with at least modest potency and that showed good discrimination between cell lines according to the following criteria: (a) average $pGI_{50} \geq 5.0$, and (b) $\max(pGI_{50}) - \min(pGI_{50}) \geq 1.5$. This resulted in 3045 compounds. We had chemical structures for 2991 of these which we designated the NCI 3K set used for the chemogenomic analysis. This is a high quality dataset showing good discrimination across the NCI-60 cell lines.

Pearson correlation coefficients were calculated to correlate gene expression profiles with patterns of compound activities across the NCI-60.

$$r_{A_iT_j} = \frac{S_{A_iT_j}}{S_{A_i}S_{T_j}}$$

where $S_{A_i}$ is activity standard deviation of *i*th compound, $S_{T_j}$ is expression standard deviation of *j*th gene, and $S_{A_iT_j}$ is covariance. Correlations were not calculated if more than one-third of the data points are missing for a given gene−compound pair; the handling of missing values was described previously.[4] In general, the six leukemia cell lines are more sensitive to cytotoxic compounds than other cell lines. The average $pGI_{50}$ value for the leukemia cell lines is $m = 5.9$ versus an average of $m = 5.0$ for the nonleukemia cell lines. Since SLC7A11 is underexpressed in leukemias,[9] a negative correlation coefficient may not be indicative of chemoresistance and may skew results. Thus, in most cases, we calculated

compound-SLC7A11 correlations using the 54 nonleukemia cell lines (denoted NCI-54).

To evaluate structure−activity relationships on the basis of correlated gene expression profiles, we clustered the NCI 3K compound set by agglomerative nesting using the complete linkage method.[53,54] The compound distance matrix, a measure of similarities or differences in chemical structures, was calculated using the Tanimoto coefficient based on the Leadscope feature set.[53] Complete linkage clustering resulted in 747 classes at the threshold distance for cluster linkage of 0.7. The largest class contained 65 podophyllotoxin analogues, and 232 compounds were in singleton classes.

For each compound class we calculated the mean compound−gene correlation. To statistically compare the correlation of individual compound class and gene with that of mean compound−gene correlation for the full NCI 3K set, *z*-score was calculated according to eq 1:

$$z = (\bar{x}_1 - \bar{x}_0)\sqrt{\frac{n_1 n_0}{s_0^2(n_0 - n_1)}} \quad (1)$$

where $\bar{x}_1$,$\bar{x}_0$ are the mean activities of the subset and full set, respectively, $n_1$ and $n_0$ are the set sizes, and $s_0^2$ is the sample variance of the full set.

To analyze the structure−activity relationships with *SLC7A11* expression, we searched for correlated compound classes, defined by similar chemical structures, in the NCI 3K anticancer agent database. Table 2 shows compound classes having high mean correlations with SLC7A11 with *z*-scores of abs($z$) ≥ 5.0. The column labeled *Class* in Table 2 shows a characterizing substructure for each compound class. This was constructed either by inspection or by the method of *macrostructure assembly* (MSA)[55] using the Leadscope software package.[29] MSA constructs discriminating substructures by reassembling common medicinal chemistry building blocks. Leadscope automatically decomposes molecules into common structural fragments such as functional groups and heterocycles when compounds are loaded into the system. MSA reassembles structural fragments in a directed way to produce larger substructures that are commonly occurring within a group of compounds or that discriminate for a biological response within the group.

To study the role of SLC7A11 in chemoresistance, we focused on compounds with strongly negative SLC7A11 correlations. Because the leukemia cell lines tend to be more sensitive to cytotoxic compounds than other cell lines which may skew results, we calculated SLC7A11 correlations using the 54 nonleukemia cell lines. Then we selected all compounds from the NCI 3K set with correlation coefficient $r < -0.3$ and bootstrap *p*-value $p < 0.05$. This filtering resulted in 471 compounds which we clustered as described above. Complete linkage clustering resulted in 180 classes with 80 singletons at the threshold distance for cluster linkage of 0.7. Table 3 shows profiles of the eight classes with *z*-scores $z < -2.0$. These classes were selected for experimental evaluation, and we requested samples from the DTP.

**Compounds.** Patulin (**21**), nanaomycin A (compound **8**), plumbagin (compound **7**), 5,8-dihydroxy-1,4-naphthoquinone (naphthazarin, compound **6**), and BSO were purchased from Sigma-Aldrich (St. Louis, MO). (*S*)-4-carboxyphenylglycine ((*S*)-4-CPG) was purchased from Tocris (Ellisville, MO). Other compounds were obtained from the National Cancer Institute's Developmental Therapeutics Program (DTP) (http://dtp.nci.nih.gov/docs/misc/available_samples/dtp_indsamples.html).

**Cell Culture.** lung cancer cell lines A549, HOP-62 and HOP-92, purchased from the Division of Cancer Treatment and Diagnosis, National Cancer Institute, National Institutes of Health (http://www.dtp.nci.nih.gov), were cultured in RPMI 1640 medium with L-glutamine, supplemented with 10% fetal bovine serum, 100 U/mL sodium penicillin G and 100 μg/mL streptomycin. Cells were grown in tissue culture flasks at 37 °C in a 5% $CO_2$ atmosphere.

**SRB Cytotoxicity Assay.** Drug potency was tested using a proliferation assay with sulforhodamine B (SRB), a protein-binding reagent (Sigma). In each experiment, 3000−4000 cells per well were seeded in 96-well plates and incubated for 24 h. Anticancer drugs were added in a dilution series in three replicates, containing either no inhibitor as control or inhibitor ((*S*)-4-CPG or BSO). For BSO, a concentration of 2.5 μM was used for A549 cells and 1 μM for HOP-62 cells; for (*S*)-4-CPG, 50 μM was used for both cell lines. For both inhibitor and control series, anticancer drugs were added in a dilution series in three replicates. After 3 days, incubation was terminated by replacing the medium with 100 μL 10% trichloroacetic acid (Sigma) in 1 × PBS, followed by incubation at 4 °C for at least 1 h. Subsequently, the plates were washed with water and air-dried. The plates were stained with 50 μL of 0.4% SRB (Sigma) in 1% acetic acid for 30 min at room temperature. Unbound dye was washed off with 1% acetic acid. After air-drying and resolubilization of the protein-bound dye in 10 mM Tris-HCl (pH 8.0), absorbance was read in a microplate reader at 570 nm, and background absorbance at 690 nm was subtracted. To determine $GI_{50}$ values, the absorbance of control cells without drug was set at 1. Dose−response curves were plotted using Prism software (San Diego, CA).

**Acknowledgment.** This work was supported in part by NIH grant GM61390.

**Supporting Information Available:** Table S1, Pearson correlations of SCL7A11 and γ-GCS with ten compounds that were sensitized more than twofold by (*S*)-4-CPG in HOP-62 cell line; Figure S1, glutathione synthesis, the glutathione redox cycle, and representative reactions involved in conjugation and detoxification; Figure S2, Comparison of compound sensitization by inhibition of SLC7A11 by (*S*)-4-CPG versus inhibition of γ-GCS by BSO in A549 cells. This material is available free of charge via the Internet at http://pubs.acs.org.

## References

(1) Weinstein, J. N.; Myers, T. G.; O'Connor, P. M.; Friend, S. H.; Fornace, A. J., Jr.; Kohn, K. W.; Fojo, T.; Bates, S. E.; Rubinstein, L. V.; Anderson, N. L.; Buolamwini, J. K.; van Osdol, W. W.; Monks, A. P.; Scudiero, D. A.; Sausville, E. A.; Zaharevitz, D. W.; Bunow, B.; Viswanadhan, V. N.; Johnson, G. S.; Wittes, R. E.; Paull, K. D. An information-intensive approach to the molecular pharmacology of cancer. *Science* **1997**, *275*, 343−9.

(2) Huang, Y.; Sadee, W. Membrane transporters and channels in chemoresistance and -sensitivity of tumor cells. *Cancer Lett.* **2006**, *239*, 168−82.

(3) Frank, N. Y.; Margaryan, A.; Huang, Y.; Schatton, T.; Waaga-Gasser, A. M.; Gasser, M.; Sayegh, M. H.; Sadee, W.; Frank, M. H. ABCB5-mediated doxorubicin transport and chemoresistance in human malignant melanoma. *Cancer Res.* **2005**, *65*, 4320−33.

(4) Huang, Y.; Blower, P. E.; Yang, C.; Barbacioru, C.; Dai, Z.; Zhang, Y.; Xiao, J. J.; Chan, K. K.; Sadee, W. Correlating gene expression with chemical scaffolds of cytotoxic agents: ellipticines as substrates and inhibitors of MDR1. *Pharmacogenomics J.* **2005**, *5*, 112−25.

(5) Huang, Y.; Anderle, P.; Bussey, K. J.; Barbacioru, C.; Shankavaram, U.; Dai, Z.; Reinhold, W. C.; Papp, A.; Weinstein, J. N.; Sadee, W. Membrane transporters and channels: role of the transportome in cancer chemosensitivity and chemoresistance. *Cancer Res.* **2004**, *64*, 4294−301.

(6) Dai, Z.; Barbacioru, C.; Huang, Y.; Sadee, W. Prediction of anticancer drug potency from expression of genes involved in growth factor signaling. *Pharm. Res.* **2006**, *23*, 336−49.

(7) Scherf, U.; Ross, D. T.; Waltham, M.; Smith, L. H.; Lee, J. K.; Tanabe, L.; Kohn, K. W.; Reinhold, W. C.; Myers, T. G.; Andrews, D. T.; Scudiero, D. A.; Eisen, M. B.; Sausville, E. A.; Pommier, Y.; Botstein, D.; Brown, P. O.; Weinstein, J. N. A gene expression database for the molecular pharmacology of cancer. *Nat. Genet.* **2000**, *24*, 236−44.

(8) Blower, P. E.; Yang, C.; Fligner, M. A.; Verducci, J. S.; Yu, L.; Richman, S.; Weinstein, J. N. Pharmacogenomic analysis: correlating molecular substructure classes with microarray gene expression data. *Pharmacogenomics J.* **2002**, *2*, 259−71.

(9) Huang, Y.; Dai, Z.; Barbacioru, C.; Sadee, W. Cystine-glutamate transporter SLC7A11 in cancer chemosensitivity and chemoresistance. *Cancer Res.* **2005**, *65*, 7446−54.

(10) Gottesman, M. M. Mechanisms of cancer drug resistance. *Annu. Rev. Med.* **2002**, *53*, 615−27.
(11) Fojo, T.; Bates, S. Strategies for reversing drug resistance. *Oncogene* **2003**, *22*, 7512−23.
(12) Calvert, P.; Yao, K. S.; Hamilton, T. C.; O'Dwyer, P. J. Clinical studies of reversal of drug resistance based on glutathione. *Chem. Biol. Interact.* **1998**, *111*−*112*, 213−24.
(13) Wu, G.; Fang, Y. Z.; Yang, S.; Lupton, J. R.; Turner, N. D. Glutathione metabolism and its implications for health. *J. Nutr.* **2004**, *134*, 489−92.
(14) Lu, S. C. Regulation of glutathione synthesis. *Curr. Top. Cell. Regul.* **2000**, *36*, 95−116.
(15) Balendiran, G. K.; Dabur, R.; Fraser, D. The role of glutathione in cancer. *Cell Biochem. Funct.* **2004**, *22*, 343−52.
(16) Sato, H.; Tamba, M.; Ishii, T.; Bannai, S. Cloning and expression of a plasma membrane cystine/glutamate exchange transporter composed of two distinct proteins. *J. Biol. Chem.* **1999**, *274*, 11455−8.
(17) Sato, H.; Tamba, M.; Kuriyama-Matsumura, K.; Okuno, S.; Bannai, S. Molecular cloning and expression of human xCT, the light chain of amino acid transport system xc. *Antioxid. Redox. Signal.* **2000**, *2*, 665−71.
(18) Sato, H.; Tamba, M.; Okuno, S.; Sato, K.; Keino-Masu, K.; Masu, M.; Bannai, S. Distribution of cystine/glutamate exchange transporter, system x(c)-, in the mouse brain. *J. Neurosci.* **2002**, *22*, 8028−33.
(19) Bannai, S.; Tateishi, N. Role of membrane transport in metabolism and function of glutathione in mammals. *J. Membr. Biol.* **1986**, *89*, 1−8.
(20) Okuno, S.; Sato, H.; Kuriyama-Matsumura, K.; Tamba, M.; Wang, H.; Sohda, S.; Hamada, H.; Yoshikawa, H.; Kondo, T.; Bannai, S. Role of cystine transport in intracellular glutathione level and cisplatin resistance in human ovarian cancer cell lines. *Br. J. Cancer* **2003**, *88*, 951−6.
(21) Patel, S. A.; Warren, B. A.; Rhoderick, J. F.; Bridges, R. J. Differentiation of substrate and non-substrate inhibitors of transport system xc(-): an obligate exchanger of L-glutamate and L-cystine. *Neuropharmacology* **2004**, *46*, 273−84.
(22) Schnelldorfer, T.; Gansauge, S.; Gansauge, F.; Schlosser, S.; Beger, H. G.; Nussler, A. K. Glutathione depletion causes cell growth inhibition and enhanced apoptosis in pancreatic cancer cells. *Cancer* **2000**, *89*, 1440−7.
(23) Lu, S. C. Regulation of hepatic glutathione synthesis. *Semin. Liver Dis.* **1998**, *18*, 331−43.
(24) Maeda, H.; Hori, S.; Ohizumi, H.; Segawa, T.; Kakehi, Y.; Ogawa, O.; Kakizuka, A. Effective, treatment of advanced solid tumors by the combination of arsenic trioxide and L-buthionine-sulfoximine. *Cell Death Differ.* **2004**, *11*, 737−46.
(25) Andringa, K. K.; Coleman, M. C.; Aykin-Burns, N.; Hitchler, M. J.; Walsh, S. A.; Domann, F. E.; Spitz, D. R. Inhibition, of glutamate cysteine ligase activity sensitizes human breast cancer cells to the toxicity of 2-deoxy-D-glucose. *Cancer Res.* **2006**, *66*, 1605−10.
(26) http://www.clinicaltrials.gov (accessed May, 2006); Identifier: NCT00005835.
(27) Townsend, D. M.; Tew, K. D. The role of glutathione-S-transferase, in anti-cancer drug resistance. *Oncogene* **2003**, *22*, 7369−75.
(28) Townsend, D. M.; Findlay, V. L.; Tew, K. D. Glutathione S-transferases as regulators of kinase pathways and anticancer drug targets. *Methods Enzymol.* **2005**, *401*, 287−307.
(29) Leadscope, Inc., Columbus OH 43215; http://www.leadscope.com. (accessed May, 2006).
(30) Holliday, J. D.; Salim, N.; Whittle, M.; Willett, P. Analysis and display of the size dependence of chemical similarity coefficients. *J. Chem. Inf. Comput. Sci.* **2003**, *43*, 819−28.
(31) Mahfoud, R.; Maresca, M.; Garmy, N.; Fantini, J. The mycotoxin patulin alters the barrier function of the intestinal epithelium: mechanism of action of the toxin and protective effects of glutathione. *Toxicol. Appl. Pharmacol.* **2002**, *181*, 209−18.
(32) Benjamini, Y.; Hochberg, Y. Controlling the false discovery rate: A practical and powerful approach to multiple testing. *J. R. Stat. Soc. B* **1995**, *57*, 289−300.
(33) Fliege, R.; Metzler, M. Electrophilic properties of patulin. N-acetylcysteine and glutathione adducts. *Chem. Res. Toxicol.* **2000**, *13*, 373−81.
(34) Dimmock, J. R.; Chamankhah, M.; Seniuk, A.; Allen, T. M.; Kao, G. Y.; Halleran, S. Synthesis and cytotoxic evaluation of some Mannich bases of alicyclic ketones. *Pharmazie* **1995**, *50*, 668−71.
(35) Dai, J.; Weinberg, R. S.; Waxman, S.; Jing, Y. Malignant cells can be sensitized to undergo growth inhibition and apoptosis by arsenic trioxide through modulation of the glutathione redox system. *Blood* **1999**, *93*, 268−77.
(36) Gartenhaus, R. B.; Prachand, S. N.; Paniaqua, M.; Li, Y.; Gordon, L. I. Arsenic trioxide cytotoxicity in steroid and chemotherapy-resistant myeloma cell lines: enhancement of apoptosis by manipulation of cellular redox state. *Clin. Cancer Res.* **2002**, *8*, 566−72.
(37) Lee, C.; Lin, Y.; Huang, M.; Lin, C.; Liu, C.; Chow, J.; Liu, H. E. Increased cellular glutathione and protection by bone marrow stromal cells account for the resistance of non-acute promylocytic leukemia acute myeloid leukemia cells to arsenic trioxide in vivo. *Leuk. Lymphoma* **2006**, *47*, 521−9.
(38) Seo, T.; Urasaki, Y.; Takemura, H.; Ueda, T. Arsenic trioxide circumvents multidrug resistance based on different mechanisms in human leukemia cell lines. *Anticancer Res.* **2005**, *25*, 991−8.
(39) Ford, J. M.; Yang, J. M.; Hait, W. N. Effect of buthionine sulfoximine on toxicity of verapamil and doxorubicin to multidrug resistant cells and to mice. *Cancer Res.* **1991**, *51*, 67−72.
(40) Nielsen, D.; Maare, C.; Skovsgaard, T. Cellular resistance to anthracyclines. *Gen. Pharmacol.* **1996**, *27*, 251−5.
(41) Bonati, A.; Rizzoli, V.; Lunghi, P. Arsenic trioxide in hematological malignancies: the new discovery of an ancient drug. *Curr. Pharm. Biotechnol.* **2006**, *7*, 397−405.
(42) Shivarama Holla, B.; Veerendra, B.; Shivananda, M. K.; Poojary, B. Synthesis characterization and anticancer activity studies on some Mannich bases derived from 1,2,4-triazoles. *Eur. J. Med. Chem.* **2003**, *38*, 759−67.
(43) Joshi, S.; Khosla, N.; Tiwari, P. In vitro study of some medicinally important Mannich bases derived from antitubercular agent. *Bioorg. Med. Chem.* **2004**, *12*, 571−6.
(44) Gul, H. I.; Sahin, F.; Gul, M.; Ozturk, S.; Yerdelen, K. O. Evaluation of antimicrobial activities of several mannich bases and their derivatives. *Arch. Pharm.* (*Weinheim*). **2005**, *338*, 335−8.
(45) Pandeya, S. N.; Sriram, D.; Nath, G.; De Clercq, E. Synthesis, antibacterial, antifungal and anti-HIV activities of norfloxacin mannich bases. *Eur. J. Med. Chem.* **2000**, *35*, 249−55.
(46) Stepkowski, S. M.; Kao, J.; Wang, M. E.; Tejpal, N.; Podder, H.; Furian, L.; Dimmock, J.; Jha, A.; Das, U.; Kahan, B. D.; Kirken, R. A. The Mannich base NC1153 promotes long-term allograft survival and spares the recipient from multiple toxicities. *J. Immunol.* **2005**, *175*, 4236−46.
(47) Monks, T. J.; Anders, M. W.; Dekant, W.; Stevens, J. L.; Lau, S. S.; van Bladeren, P. J. Glutathione conjugate mediated toxicities. *Toxicol. Appl. Pharmacol.* **1990**, *106*, 1−19.
(48) Dekant, W.; Vamvakas, S. Glutathione-dependent bioactivation of xenobiotics. *Xenobiotica* **1993**, *23*, 873−87.
(49) Kandepu NM, Ph.D. Dissertation, http://library.usask.ca/theses/available/etd-10212004−002012/(accessed May, 2006).
(50) Chen, X.; Carystinos, G. D.; Batist, G. Potential for selective modulation of glutathione in cancer chemotherapy. *Chem. Biol. Interact.* **1998**, *111*−*112*, 263−75.
(51) Sugiyama, T.; Sadzuka, Y. Theanine and glutamate transporter inhibitors enhance the antitumor efficacy of chemotherapeutic agents. *Biochim. Biophys. Acta* **2003**, *1653*, 47−59.
(52) Data kindly provided by Mark Reimers, Laboratory of Molecular Pharmacology, National Cancer Institute, National Institutes of Health, Bethesda, MD 20892.
(53) Blower, P. E., Jr.; Cross, K. P.; Fligner, M. A.; Myatt, G. J.; Verducci, J. S.; Yang, C. Systematic analysis of large screening sets in drug discovery. *Curr. Drug Discovery Technol.* **2004**, *1*, 37−47.
(54) Everitt, B. S. *Cluster Analysis*; Halsted Press: New York, 1993.
(55) Cross, K. P.; Myatt, G.; Yang, C.; Fligner, M. A.; Verducci, J. S.; Blower, P. E., Jr. Finding discriminating structural features by reassembling common building blocks. *J. Med. Chem.* **2003**, *46*, 4770−5.

JM060960H